Yet another representation of $SO(3)$ by spherical functions for pose estimation

Toru Tamaki† Toshiyuki Amano‡ Kazufumi Kaneda

†: Hiroshima University, Japan ‡: NAIST, Japan

Abstract We propose a novel representation of $SO(3)$ pose in 3 degrees-of-freedom (DOF) for view-based pose estimation. First we show that a conventional representation of pose in 1 DOF is a Fourier basis, and extend the observation to 2 DOF with spherical harmonics. Then we represent 3 DOF pose with spherical functions that are continuous orthonormal basis on $SO(3)$, and give transformations from the spherical functions representation to a quaternion and a rotation matrix.

1 Introduction

What is a pose? It is an important question for estimating parameters of poses. In computer vision with three-dimensional geometry, a rotation matrix R, that transforms the world coordinate system to a camera or object coordinate system, is called a pose of a camera or an object.

To see a pose for estimation, we focus on a method for global appearance-based (view-based) pose estimation. It can be seen as regression that learns relations between images (views or appearances) and pose parameters. A training set $\{p_j, \boldsymbol{x}_j\}_{j=1,2,\ldots}$ is given where p_j is a parameter vector of a pose and $\boldsymbol{x}_j$ is an image vector corresponding to the pose. In training phase, the relation $p_j = f(\boldsymbol{x}_j)$ between them is learned. In test phase, a pose p of a test image $\boldsymbol{x}$ is estimated as $p = f(\boldsymbol{x})$.

In this paper, we propose a novel representation of a pose of an object under a 3 degrees-of-freedom (DOF) rotation, that is, a rotation in $SO(3)$. There have not been any considerations on a representation of a pose $\boldsymbol{p}$ for pose estimation, whereas many estimation methods f have been studied. However, we have to carefully choose an appropriate pose representation because of problems specific to 3 DOF pose estimation.

There are three types of rotations specified by DOF (see Fig. 1). In 1 DOF rotation, an object rotates about an axis by an angle $\theta_1 \in [0, 2\pi)$ that can be uniquely determined by the angle between a point on a unit circle $S^1 = \{\boldsymbol{p} \in \mathbb{R}^2 \mid ||\boldsymbol{p}|| = 1\}$ and the reference point ($\theta_1 = 0$). In 2 DOF, an object rotates about two axes with angles θ_1, θ_2 such as azimuth, zenith, or elevation. These angles are

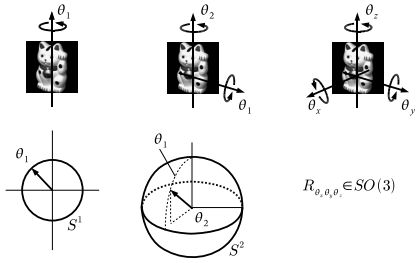

Fig. 1: 1,2,3 DOF rotations

uniquely determined by a point on a unit sphere $S^2 = \{\boldsymbol{p} \in \mathbb{R}^3 \mid ||\boldsymbol{p}|| = 1\}$. In 3 DOF, an object rotates about three orthogonal axes (e.g., x, y, z) by angles $\theta_x, \theta_y, \theta_z$ which are called roll–pitch–yow or Euler angles [1]. Because of their ambiguity [2], a 3 DOF pose is uniquely determined by a 3×3 rotation matrix R with its reference, an identity matrix I. R is an element of the special orthogonal group $SO(3) = \{R \in \mathbb{R}^{3\times3} \mid RR^T = R^TR = I, \det(R) = 1\}$.

Previous works on 1 DOF pose estimation have focused mainly on an estimation method f which relates an image $\boldsymbol{x}$ and a pose $\boldsymbol{p}$: linear methods [3, 4, 5], kernel or non-linear methods [6, 7, 8, 9], non-function procedure [10]. These works do not pay any attention on whether a pose representation is appropriate or not.

We focus on an appropriate representation of 3 DOF pose for linear pose estimation methods. Separating pose representation from estimation methodology enables us to apply the representation to any estimation method.

The organization of the paper is as follows. In section 2 and 3, we discuss requirements for repre-

sentations for 1 DOF and 2 DOF pose estimations. Then, we propose new representations for 3 DOF pose in section 4. In section 5, we show experimental results of pose estimation.

2 1 DOF pose representation

2.1 Previous representation

Here we review a representation used by works on 1 DOF pose estimation [3, 8, 9, 7, 6, 4]. In training phase, images $\boldsymbol{x}_j \in \mathbb{R}^N$ of an object rotating about an axis and corresponding angles $\theta_{1j} \in [0, 2\pi)$ are given. A pose is represented by a vector $\boldsymbol{p}_j = (\cos\theta_{1j}, \sin\theta_{1j})^T \in \mathbb{R}^2$ such that the following constraint is satisfied:

$$(\boldsymbol{p}_1, \boldsymbol{p}_2, \ldots, \boldsymbol{p}_n) = F(\boldsymbol{x}_1, \boldsymbol{x}_2, \ldots, \boldsymbol{x}_n), \tag{1}$$

where a matrix $F \in \mathbb{R}^{2\times N}$ is estimated.

In test phase, the pose of a given image $\boldsymbol{x}$ is estimated as $F\boldsymbol{x} = \hat{\boldsymbol{p}} = (\hat{p}_1, \hat{p}_2)^T$, then the angle is retrieved as $\hat{\theta}_1 = \tan^{-1}\frac{\hat{p}_2}{\hat{p}_1}$ even if $\hat{\boldsymbol{p}}$ may not be on a unit circle. In practice, `atan2()` is used.

By observing the representation above, we claim that any pose representation should have two properties: continuity and bijection.

2.2 Continuity

The angle θ_1 is never used to represent a 1 DOF pose because the angle have discontinuity at 2π.

It is well known that we can assume that images belonging to a training class can be approximated by a linear combination of eigenvectors in the class. Because an eigenspace spanned by eigenvectors are contained by a space spanned by training images of the class, we can approximate an image $\boldsymbol{x}$ by a linear combination of training samples:

$$\boldsymbol{x} \cong b_1\boldsymbol{x}_1 + b_2\boldsymbol{x}_2 + \cdots + b_n\boldsymbol{x}_n. \tag{2}$$

On the other hand, the pose $\boldsymbol{p}_j$ of a training image $\boldsymbol{x}_j$ is mapped by a linear function (matrix) F to the pose $\boldsymbol{p}_j$

$$\boldsymbol{p}_j \cong F\boldsymbol{x}_j. \tag{3}$$

Therefore, we have the following equation:

$$\begin{aligned} \boldsymbol{p} = F\boldsymbol{x} &= b_1F\boldsymbol{x}_1 + b_2F\boldsymbol{x}_2 + \cdots + b_nF\boldsymbol{x}_n & (4)\\ &\cong b_1\boldsymbol{p}_1 + b_2\boldsymbol{p}_2 + \cdots + b_n\boldsymbol{p}_n, & (5)\end{aligned}$$

which means that the estimated pose $\boldsymbol{p}$ is also a linear combination of poses $\boldsymbol{p}_j$ of training images.

o

A problem happens if a pose representation has discontinuity. For example, poses $0, 5, \ldots, 300, 350$ ° are learned with the angle θ_1. Then, an estimate of a pose for 355° might be a linear combination of 350° and 0° , which results in 175° . The same problem occurs even for kernel based methods [7].

Therefore, each parameter in a representation $\boldsymbol{p}$ is required to be (at least C^1) continuous with pose.

2.3 Bijection

Second property is bijection: the mapping between an image $\boldsymbol{x}$ and a pose $\boldsymbol{p}$ should be a one-to-one and onto mapping.

Pose estimation can not be performed with a non-bijective representation. If an image $\boldsymbol{x}$ has two pose representations $\boldsymbol{p}_1$ and $\boldsymbol{p}_2$, no linear mapping F satisfies both $F\boldsymbol{x} = \boldsymbol{p}_1$ and $F\boldsymbol{x} = \boldsymbol{p}_2$.

The relation between $\cos, \sin$ and a point on a unit circle is bijective. However, the angle θ_1 is not because θ_1 and $\theta_1 + 2n\pi$ $(n \in \mathbb{Z})$ indicate the same pose.

2.4 Representing pose by Fourier basis

According to the discussion above, we have the following statement: *a pose of 1 DOF is represented by periodical C^1-continuous functions $C^1(S^1)$ defined on a unit circle S^1.*

Candidates of such functions are the complex Fourier basis, C^∞-continuous periodic functions defined on S^1:

$$Y_{\ell_1} = e^{-\ell_1\theta_1 i},\ \ell_1 \in \mathbb{Z}, \quad i = \sqrt{-1}, \tag{6}$$

which can approximate any functions in $C^\infty(S^1)$.

Therefore, the representation $(\cos\theta_{1j}, \sin\theta_{1j})^T$ can be regard as the real and imaginary parts of the lowest frequency $Y_{\pm 1} = e^{\pm\theta_1 i}$.

3 2 DOF pose representation

Now we consider a pose representation of 2 DOF in the same manner: use the lowest frequency function for expanding a periodic continuous function $C^\infty(S^2)$ defined on a sphere S^2.

Spherical harmonics [11, 12, 13, 14] is well known as a basis for continuous functions on a sphere:

$$Y_{\ell_1,\ell_2} = \sqrt{b_{\ell_1,\ell_2}}\ P_{\ell_1}^{\ell_2}(\cos\theta_1)\ e^{-\ell_2\theta_2 i}, \quad \ell_1, \ell_2 \in \mathbb{Z}, \tag{7}$$

where $\theta_1 \in [0, \pi)$, $\theta_2 \in [0, 2\pi)$. $\ell_1 \geq |\ell_2|$, $P_{\ell_1}^{\ell_2}$ are associated Legendre polynomials, and b_{ℓ_1,ℓ_2} are coefficients. Note that we omit parameters of functions (θ_1, θ_2) for simplicity.

The lowest frequency functions are

$$Y_{1,0} = \sqrt{3}\cos\theta_1, \quad (8)$$

$$Y_{1,\pm1} = -\sqrt{\frac{3}{2}}\sin\theta_1 e^{\mp\theta_2 i}, \quad (9)$$

and inversely angles are calculated as:

$$\theta_2 = \tan^{-1}\left(\frac{-(Y_{1,-1}-Y_{1,1})/i}{-(Y_{1,-1}+Y_{1,1})}\right), \quad (10)$$

$$\theta_1 = \tan^{-1}\left(\frac{(Y_{1,-1}-Y_{1,1})/(-\sqrt{2}\ i\sin\theta_2)}{Y_{1,0}}\right). \quad (11)$$

Therefore, we can use $\boldsymbol{Y} = (Y_{1,0},\ Y_{1,1},\ Y_{1,-1})^T \in C^\infty(S^2)^3$ as a 2 DOF pose representation because they are all continuous on a sphere.

A representation of 2 DOF pose usually used is $\boldsymbol{p} = (\theta_1, \theta_2)^T$. This is not continuous at poles of a sphere and not appropriate as a pose representation. However, no problem have reported yet because the discontinuity has been ignored in experiments in small range of pose variation.

4 A new 3 DOF pose representation with spherical functions

In this section, we propose a new representation of 3 DOF pose by using continuous functions on $SO(3)$ to uniquely determine a pose.

4.1 Other representations of 3 DOF pose

There are several common representations of 3 DOF pose, but they do not satisfy the requirements; continuity and bijection.

Euler angles or fixed angles (roll–pitch–yaw) [1] have singularities and therefore not continuous. Moreover, they are not bijection because of the gimbal lock problem: angles suddenly change as a pose changes smoothly.

In angle–axis or Exponential map [15, 16], a rotation axis is represented by two opposite directions. Therefore it is not bijective. Also a rotation angle is not continuous.

Unit quaternions are continuous, but not bijection because q and $-q$ represent the same pose. Unit quaternions have been used for robot control, pose interpolation [17, 18] in CG [2, 19, 20], or 3D registration [21]. Unit quaternions are useful because of its continuity, however, bijection is also necessary for pose estimation. Unfortunately, unit quaternions are not bijective.

A 3×3 rotation matrix satisfies the requirements. R is continuous and bijective because $SO(3)$ is a smooth closed manifold. But usually it is not used for pose interpolation.

4.2 Pose representation by spherical functions

Here we use spherical functions for a pose representation. Spherical functions [22] $Y_{\ell_1,\ldots,\ell_n}$ are orthonormal C^∞-continuous basis functions on a hyper-sphere S^n. For $n = 1$ they are the complex Fourier basis Y_{ℓ_1} and for $n = 2$ the spherical harmonics Y_{ℓ_1,ℓ_2}.

Spherical functions on S^3 are as follows:

$$Y_{\ell_1,\ell_2,\ell_3} = \sqrt{b_{\ell_1,\ell_2,\ell_3}} C^{1,\ell_2}_{\ell_1}(\cos\theta_1) P^{\ell_3}_{\ell_2}(\cos\theta_2) e^{-\ell_3\theta_3 i}, \quad (12)$$

where $C^{1,\ell_2}_{\ell_1}$ are associated Gegenbauer functions. However, S^3 is a double-covering of $SO(3)$ [15, p.41], and these are not appropriate to our case.

Now we propose a representation using the lowest frequency functions of spherical functions $Y_{2\ell_1,\ell_2,\ell_3}$ on $SO(3)$ [22]. Those corresponding to the lowest frequency ($2\ell_1 = 2$) are the following 9 functions:

$$Y_{2,0,0} = 1 + 2\cos 2\theta_1 \quad (13)$$

$$Y_{2,1,0} = \sqrt{24}\sin\theta_1\cos\theta_1\cos\theta_2 \quad (14)$$

$$Y_{2,1,\pm1} = -2\sqrt{3}\sin\theta_1\cos\theta_1\sin\theta_2 e^{\mp\theta_3 i} \quad (15)$$

$$Y_{2,2,0} = \sqrt{2}\sin^2\theta_1(3\cos^2\theta_2 - 1) \quad (16)$$

$$Y_{2,2,\pm1} = -2\sqrt{3}\sin^2\theta_1\sin\theta_2\cos\theta_2 e^{\mp\theta 3i} \quad (17)$$

$$Y_{2,2,\pm2} = \sqrt{3}\sin^2\theta_1\sin^2\theta_2 e^{\mp 2\theta 3i} \quad (18)$$

For simplicity, we modify the functions as follows:

$$Y_0 = 4\cos{\theta_1}^2 - 1 \quad (19)$$

$$Y_1 = \cos\theta_1\sin\theta_1\cos\theta_2 \quad (20)$$

$$Y_2 = \cos\theta_1\sin\theta_1\sin\theta_2\cos\theta_3 \quad (21)$$

$$Y_3 = \cos\theta_1\sin\theta_1\sin\theta_2\sin\theta_3 \quad (22)$$

$$Y_4 = \sin^2\theta_1(3\cos^2\theta_2 - 1) \quad (23)$$

$$Y_5 = \sin^2\theta_1\cos\theta_2\sin\theta_2\cos\theta_3 \quad (24)$$

$$Y_6 = \sin^2\theta_1\cos\theta_2\sin\theta_2\sin\theta_3 \quad (25)$$

$$Y_7 = \sin^2\theta_1\sin^2\theta_2(\cos^2\theta_3 - \sin^2\theta_3) \quad (26)$$

$$Y_8 = \sin^2\theta_1\sin^2\theta_2\cos\theta_3\sin\theta_3 \quad (27)$$

We call $\boldsymbol{Y} = (Y_0, Y_1, \ldots, Y_8)^T$ *a spherical function representation of pose.*

4.3 Conversions to other representations

We give some conversions of the spherical function representation to and from other representations.

A point $\boldsymbol{q} = (q_1, q_2, q_3, q_4)^T$ on a sphere S^3 is

$$\boldsymbol{q} = (\cos\theta_1,\ \sin\theta_1\cos\theta_2 \sin\theta_1\sin\theta_2\cos\theta_3,\ \sin\theta_1\sin\theta_2\sin\theta_3)^T. \quad (28)$$

By using the elements of $\boldsymbol{q}$ above, the spherical function representation can be rewritten as follows:

$$\boldsymbol{Y} = (4q_1^2 - 1,\ q_1q_2,\ q_1q_3,\ q_1q_4,\ 3q_2^2 - 1 + q_1^2,\ q_2q_3,\ q_2q_4,\ q_3^2 - q_4^2,\ q_3q_4)^T, \tag{29}$$

and inversely,

$$(q_1^2,\ q_2^2,\ q_3^2,\ q_4^2) = \left(\tfrac{Y_0+1}{4}, \tfrac{Y_0-4Y_4-3}{-12}, \tfrac{Y_0+2Y_4-6Y_7-3}{-12}, \tfrac{Y_0+2Y_4+6Y_7-3}{-12}\right). \tag{30}$$

Note that $q_1^2 + q_2^2 + q_3^2 + q_4^2 = 1$ is hold and it is indeed a unit quaternion. $\boldsymbol{Y}$ corresponds to both $\boldsymbol{q}$ and $-\boldsymbol{q}$ because signs are ignored.

Now, we define quaternion operations on points on S^3 and then identify $\boldsymbol{q}$ with a unit quaternion q. This means that θ_2, θ_3 are angles of an axis, and θ_1 is the angle about the axis of a rotation represented by q.

A conversion between a unit quaternion q and a rotation matrix R_q is well known [19]:

$$R_q = \begin{pmatrix} q_1^2 + q_2^2 - q_3^2 - q_4^2 & 2q_2q_3 - 2q_1q_4 & 2q_2q_4 + 2q_1q_3 \\ 2q_2q_3 + 2q_1q_4 & q_1^2 - q_2^2 + q_3^2 - q_4^2 & 2q_3q_4 - 2q_1q_2 \\ 2q_2q_4 - 2q_1q_3 & 2q_3q_4 + 2q_1q_2 & q_1^2 - q_2^2 - q_3^2 + q_4^2 \end{pmatrix}. \tag{31}$$

Using this formula, the spherical function representation is converted to a rotation matrix as follows:

$$R_{\boldsymbol{Y}} = \begin{pmatrix} \frac{Y_0+2Y_4}{3} & 2Y_5 - 2Y_3 & 2Y_6 + 2Y_2 \\ 2Y_5 + 2Y_3 & \frac{Y_0-Y_4+3Y_7}{3} & 2Y_8 - 2Y_1 \\ 2Y_6 - 2Y_2 & 2Y_8 + 2Y_1 & \frac{Y_0-Y_4-3Y_7}{3} \end{pmatrix}. \tag{32}$$

5 Experimental results

We describe experimental results with images for pose estimation by using the proposed spherical function representation and the other (unit quaternions and a rotation matrix) representation.

5.1 Setup

We used Dwarf images [23] in which an object is fixed at the center of a view hemisphere (see Fig. 2(a)) and cameras are placed at grids on the hemisphere. The number of images is 2500 by varying 100 azimuth angles $\phi^x = 0 \sim 360$ ° and 25 elevation angles $\phi^y = 0 \sim 90$ ° by 3.6 ° . The reference

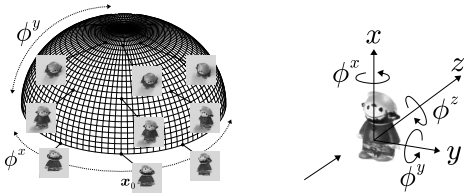

(a) (b)

Fig. 2: Dwarf images [23] used by experiments. (a) Camera positions. (b) Correspondence between Dwarf images and rotation axes.

camera position $\phi^x = \phi^y = 0$ ° corresponds to $\boldsymbol{x}_0$ in the figure.

30 images with $\phi^x = 0, 36, 72, \ldots, 324$ ° and $\phi^y = 0, 36, 72$ ° are used for training. 2470 images are used for testing: $\phi^x = 0, 3.6, 7.2, \ldots$ ° and $\phi^y = 0, 3.6, 7.2, \ldots$ ° , except 30 training images.

5.2 Pose parameterization

We parameterized the pose as shown in Fig. 2(b). Instead of using the hemisphere, we can see view changes as rotations of the object by angles ϕ^x, ϕ^y, ϕ^z about x, y, z axes.

Then, we define a pose of an image $\boldsymbol{x}_j$ by a unit quaternion q_j:

$$\begin{aligned} q_j^x &= \cos(\phi_j^x/2) + \sin(\phi_j^x/2)(\mathsf{i} + 0\mathsf{j} + 0\mathsf{k}) && (33)\\ q_j^y &= \cos(\phi_j^y/2) + \sin(\phi_j^y/2)(0\mathsf{i} + \mathsf{j} + 0\mathsf{k}) && (34)\\ q_j^z &= \cos(\phi_j^z/2) + \sin(\phi_j^y/2)(0\mathsf{i} + 0\mathsf{j} + \mathsf{k}) && (35)\\ q_j &= q_j^z q_j^y q_j^x && (36) \end{aligned}$$

because a unit quaternion of a rotation by an angle θ about an axis $\boldsymbol{n} = (n_1, n_2, n_3)^T$ is given by[2]

$$q = \cos(\theta/2) + \sin(\theta/2)(n_1\mathsf{i} + n_2\mathsf{j} + n_3\mathsf{k}), \quad ||\boldsymbol{n}|| = 1. \tag{37}$$

5.3 Estimation method

We used the most simple one for estimation: a linear regression [3]. Training images $\boldsymbol{x}_j$ and its corresponding poses $\boldsymbol{Y}_j$

$$Y = (\boldsymbol{Y}_1, \boldsymbol{Y}_2, \ldots, \boldsymbol{Y}_n), \quad X = (\boldsymbol{x}_1, \boldsymbol{x}_2, \ldots, \boldsymbol{x}_n), \tag{38}$$

are used to calculate a matrix F such that $Y = FX$ is satisfied: therefore, $F = YX^+ = Y(X^TX)^{-1}X^T$ where X^+ is the pseudo-inverse of X.

An estimate $\hat{\boldsymbol{Y}}$ of an image $\boldsymbol{x}$ is given by $\hat{\boldsymbol{Y}} = F\boldsymbol{x}$.

5.4 Representations to compare

To compare the difference of estimates of different representations, estimates of different representa-

Table 1: RMSE for each representation

	$R_{\bar{\boldsymbol{q}}}$	$R_{\hat{\boldsymbol{q}}}$	$\bar{R}$	$\hat{R}$	$R_{\hat{\boldsymbol{Y}}}$
RMSE	1.1514	1.0460	0.7414	0.7032	0.7032
std.	2.0635	1.2306	1.3812	0.7901	0.7901

tions were converted to rotation matrices as the following procedures.

- Train a spherical function representation $\boldsymbol{Y}_j \in \mathbb{R}^9$. An estimate $\hat{\boldsymbol{Y}}$ is converted to a rotation matrix $R_{\hat{\boldsymbol{Y}}}$.
- Train a vector $\boldsymbol{q}_j \in \mathbb{R}^4$ of a unit quaternion q_j. An estimate $\hat{\boldsymbol{q}}$ is normalized as $\bar{\boldsymbol{q}} = \frac{\hat{\boldsymbol{q}}}{||\hat{\boldsymbol{q}}||}$, then converted to a rotation matrix $R_{\bar{\boldsymbol{q}}}$.
- Train a vector $\boldsymbol{R}_j \in \mathbb{R}^9$ with rearranged elements of a rotation matrix R_j. An estimate $\hat{\boldsymbol{R}}$ is rearranged again to a matrix $\hat{R}$, then corrected to a rotation matrix $\bar{R}$ with the polar decomposition.

5.5 Error evaluation

We evaluated the error of estimates by using root mean square error (RMSE) with Frobenius norm between a true rotation matrix R^{true} and an estimated rotation matrix R:

$$||R - R^{\text{true}}||_F = \sqrt{\sum_{i=1}^{3}\sum_{j=1}^{3}(r_{ij} - r_{ij}^{\text{true}})^2}. \quad (39)$$

RMSE was computed for 2470 test images.

5.6 Results

Table 1 shows RMSE of pose estimation with each pose representation. $R_{\hat{\boldsymbol{Y}}}$ is small, which shows the proposed spherical representation is useful for this application.

$\hat{R}$ shows the result of a rotation matrix as representation except the matrix correction, which means that $\hat{R}$ is not rotation. With the correction, $\bar{R}$ is a rotation but the error increases.

Note that $\hat{R}$ and $R_{\hat{\boldsymbol{Y}}}$ are identical because of the linearity of the regression. Therefore, both can use the same matrix correction to make them rotation matrices.

$R_{\bar{\boldsymbol{q}}}$ shows the results of a unit quaternion. It is a rotation matrix but the error is larger than the other representations, as large as $R_{\hat{\boldsymbol{q}}}$ without normalization.

6 Conclusions

We have proposed a new pose representation of 3 DOF rotation. The proposed spherical function representation uses a continuous orthonormal basis of functions on $SO(3)$. We have shown the conversions of the proposed representation to other representations such as a unit quaternions and a rotation matrix. In experiments, we have shown that the proposed representation is identical to a rotation matrix, and it is better than results of unit quaternions.

Future work includes the extension to higher order error analysis with the proposed representation. Unlike a rotation matrix, spherical functions have higher order (higher frequency) functions that are not used here. Error functions defined on $SO(3)$ usually appear in many computer vision problems such as 3D registration and multi-view geometry. The proposed representation might have successful applications as an analyzing tool of them.

References

[1] J. J. Craig, *Introduction to Robotics: Mechanics and Control*. Prentice Hall, 3 ed., 2004.

[2] A. S. Glassner, ed., *Graphics Gems*. Academic Press, 1990.

[3] T. Okatani and K. Deguchi, "Yet another appearance-based method for pose estimation based on a linear model," *IAPR Workshop on Machine Vision Applications 2000*, pp. 258–261, 2000. http://b2.cvl.iis.u-tokyo.ac.jp/mva/proceedings/CommemorativeDVD/2000/papers/2000258.pdf.

[4] T. Amano and T. Tamaki, "An appearance based fast linear pose estimation," *IAPR Conference on Machine Vision Applications 2009*, pp. 182–186, 2009. http://ir.lib.hiroshima-u.ac.jp/metadb/up/ZZT00003/MVA2009_06-03.pdf.

[5] T. Tamaki, T. Amano, and K. Kaneda, "Representing images of a rotating object with cyclic permutation for view-based pose estimation," *Computer Vision and Image Understanding*, vol. 113, no. 12, pp. 1210 – 1221, 2009. http://www.sciencedirect.com/science/article/B6WCX-4X1YCMF-1/2/b01ba9a647b5b09dad88b49ed8a64cb4.

[6] S. Ando, Y. Kusachi, A. Suzuki, and K. Arakawa, "Appearance based pose estimation of 3D object using support vector regression," *ICIP2005*, vol. 1, pp. I–341–344, 2005. http://ieeexplore.ieee.org/xpls/abs_all.jsp?arnumber=1529757&isnumber=32660.

[7] T. Melzer, M. Reiter, and H. Bischof, "Appearance models based on kernel canonical correlation analysis," *Pattern Recognition*, vol. 36, pp. 1961–1971, 2003. http://dx.doi.org/10.1016/S0031-3203(03)00058-X.

[8] T. Sun and S. Chen, "Locality preserving CCA with applications to data visualiza-

tion and pose estimation," *Image and Vision Computing*, vol. 25, no. 5, pp. 531–543, 2007. http://www.sciencedirect.com/science/article/B6V09-4K9C6GM-2/2/a1930d130b2c0f9fec65465579d50d11.

[9] S. Fidler, D. Skočaj, and A. Leonardis, "Combining reconstructive and discriminative subspace methods for robust classification and regression by subsampling," *IEEE Trans. on Pattern Analysis and Machine Intelligence*, vol. 28, no. 3, pp. 337–350, 2006. http://doi.ieeecomputersociety.org/10.1109/TPAMI.2006.46.

[10] H. Murase and S. K. Nayar, "Visual learning and recognition of 3-D objects from appearance," *International Journal of Computer Vision*, vol. 14, no. 1, pp. 5–24, 1995. http://dx.doi.org/10.1007/BF01421486.

[11] I. Sato, Y. Sato, and K. Ikeuchi, "Illumination from shadows," *IEEE Trans. on Pattern Analysis and Machine Intelligence*, vol. 25, no. 3, pp. 290–300, 2003. http://doi.ieeecomputersociety.org/10.1109/TPAMI.2003.1182093.

[12] P.-M. Lam, C.-S. Leung, and T.-T. Wong, "Noise-resistant fitting for spherical harmonics," *IEEE Trans. Visualization and Computer Graphics*, vol. 12, no. 2, pp. 254–265, 2006. http://doi.ieeecomputersociety.org/10.1109/TVCG.2006.34.

[13] T. Okabe, I. Sato, and Y. Sato, "Spherical harmonics vs. haar wavelets: basis for recovering illumination from cast shadows," *CVPR2004*, vol. 1, pp. 50–57, 2004. http://www.hci.iis.u-tokyo.ac.jp/~okabe/okabe-CVPR04.pdf.

[14] R. Lenz, *Group Theoretical Methods in Image Processing*, vol. 413 of *Lecture Notes in Computer Science*. Springer Verlag, 1990. http://staffwww.itn.liu.se/~reile/LNCS413/index.htm.

[15] Y. Ma, S. Soatto, J. Košecká, and S. S. Sastry, *An Invitation To 3-D Vision*. Springer, 2004. http://vision.ucla.edu/MASKS/.

[16] F. S. Grassia, "Practical parameterization of rotations using the exponential map," *Journal of Graphics Tools*, vol. 3, no. 3, pp. 29–48, 1998. http://jgt.akpeters.com/papers/Grassia98/.

[17] F. C. Park and B. Ravani, "Smooth invariant interpolation of rotations," *ACM Trans. Graph.*, vol. 16, no. 3, pp. 277–295, 1997. http://doi.acm.org/10.1145/256157.256160.

[18] K. Shoemake, "Animating rotation with quaternion curves," *SIGGRAPH'85*, vol. 19, no. 3, pp. 245–254, 1985. http://doi.acm.org/10.1145/325165.325242.

[19] A. J. Hanson, "Visualizing quaternions," in *SIGGRAPH '05: ACM SIGGRAPH 2005 Courses*, ACM, 2005. http://doi.acm.org/10.1145/1198555.1198701.

[20] J. C. Hart, G. K. Francis, and L. H. Kauffman, "Visualizing quaternion rotation," *ACM Trans. Graph.*, vol. 13, no. 3, pp. 256–276, 1994. http://doi.acm.org/10.1145/195784.197480.

[21] R. Benjemaa and F. Schmitt, "A solution for the registration of multiple 3D point sets using unit quaternions," *Proc. of ECCV98*, vol. 2, pp. 34–50, 1998. http://www.tsi.enst.fr/publications/Benjemaa/eccv98.ps.gz.

[22] M. Takeuchi, *Modern Spherical Functions*. American Mathematical Society, 1994.

[23] G. Peters, B. Zitova, and C. von der Malsburg, "How to measure the pose robustness of object views," *Image and Vision Computing*, vol. 20, no. 4, pp. 249–256, 2002. http://ls7-www.cs.uni-dortmund.de/~peters/pages/research/modeladaptsys/modeladaptsys_vba_rov.html.